Hydrogen Production from Bioinspired Methanol Reforming at Room Temperature

Yangbin Shen,[*,a] Ziwen Xu,[a] Luqi Wang,[a] and Yulu Zhan,[*b]*

[a]Institute of Materials Science and Devices, Suzhou University of Science and Technology, Suzhou 215009, China

[b] Beijing National Laboratory for Molecular Sciences, College of Chemistry and Molecular Engineering, Peking University, Beijing 100871, China

Keywords: Hydrogen Production; Methanol-Water Reforming; Ruthenium Metal-Organic Frameworks; Bio-induced Reaction.

Contents

SI-1. Chemicals and Materials.

All chemicals are commercial and used without further purification unless specified. Alcohol dehydrogenase from Saccharomyces cerevisiae (ADH 331 units/mg solid, molecular weight of ADH (M_{ADH}) =141 kDa, Sigma-Aldrich Co. LLC.), β-Nicotinamide adenine dinucleotide hydrate (NAD^+,$C_{21}H_{27}N_7O_{14}P_2$, Sigma-Aldrich Co. LLC.,>99%), β-Nicotinamide adenine dinucleotide, reduced disodium salt hydrate (NADH, J&K Scientific Ltd,98%),ethanol (C_2H_5OH, Tianjing Baishi Chemical Industry Co., Ltd, >99.7%), 3,3',5,5'-tetramethylbenzidine (TMB) ($C_{16}H_{20}N_2$, Shanghai Aladdin Biochemical Technology Co., Ltd, >99%), sodium hydroxide (NaOH, Sinopharm Chemical Reagent, Co., Ltd, >96%) , dichloro(p-cymene)ruthenium(II) dimer ($C_{20}H_{28}Cl_4Ru_2$, Energy Chemical Reagent. Co., Ltd., 98%), formaldehyde (HCHO, Shanghai Lingfeng Chemical Reagent. Co., Ltd, 37%), disodium hydrogen phosphate (Na_2HPO_4, Sinopharm Chemical Reagent. Co., Ltd. >99%), sodium phosphate monobasic (NaH_2PO_4, Sinopharm Chemical Reagent. Co., Ltd. >99%), ultrapure water is prepared by Thermo PureLab Ultra Genetic.

One unit (U) is defined as the amount of the enzyme that catalyzes the conversion of 1 micro mole (μmole) of substrate per minute. For example, one unit of ADH could convert 1.0 μmole of ethanol to acetaldehyde per min at pH 8.8 at 25 ℃.

SI-2. Characterization and Physical Measurements.

Gas chromatography experiments were performed on GC-G5 chromatograph with FID/TCD and methanizer (Beijing Persee General Instrument Co., Ltd). The system used N_2 as a carrier gas, allowed for the detection limits of the following gases: $H_2 \geq 100$ ppm, CO ≥ 1 ppm. ^{1}H NMR spectra of catalysts were recorded on Varian Plus 400 MHz. The scanning electron microscope images (SEM) were recorded on Inspect F50, FEI. The transmission electron microscopy (TEM) and high resolution transmission electron microscopy (HRTEM) images were recorded on Talos F200X, Thermo Scientific. UV-absorption and enzymatic reaction kinetics were record by Shimadzu UV-2600. Powder X-ray diffraction (XRD) patterns of samples were recorded with Bruker D8 X-ray diffractometer using Cu-Kα radiation (40 kV and 10 mA). The XPS analysis was determined by Escalab 250Xi spectrometer. The ruthenium contents of the catalysts were determined by Agilent 720 ICP-OES. The FTIR data were detected by Nicolet iS10 (Nicolet Instrument Co. USA). The surface areas of the Ru-MOFs were determined by the Brunauer-Emmett-Teller (BET) method, based on the amount of N_2 adsorbed at pressures $0.005 < P/P_0 < 0.998$. The pore size distributions and average pore diameter of the catalyst were analyzed by the BJH nitrogen adsorption and desorption method (Beijing Builder Electronic Technology CO.,LTD).

SI-3. Preparation and Characterization of the Ru-MOFs.

The functional ruthenium metal organic frameworks (Ru-MOFs) was prepared through the coordination reaction of the $[Ru(p\text{-}Cymene)Cl_2]_2$ and 3,3',5,5'-tetramethylbenzidine (TMB). Typically, 48 mg TMB (0.2 mmol) was dissolved in 20 mL ethanol at 70℃, then transferred 122 mg dichloro(p-cymene)ruthenium(II) dimer (0.2 mmol) in the TMB solution. The TMB and dichloro(p-cymene)ruthenium(II) dimer are both dissolved in the ethanol at the beginning of the reaction at 70℃. The reaction solution keep stirring for 12 hours at 70℃, the yellow insoluble powder will be produced slowly during the reaction. The yellow suspension was filtered by the filter membrane and washed with hot ethanol. At last, we could gain the Ru-MOFs after the yellow powder was dried under vacuum. The preparation process was as follows.

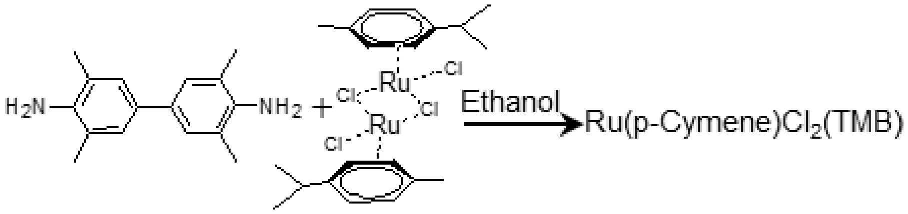

Scheme S 1. Schematic Illustration for the Ru-MOFs Preparation.

Characterization of the Ru-MOFs.

The XPS measurements were employed via Escalab 250Xi spectrometer. The main elements in the Ru-MOFs is Ru, C, N and Cl after the XPS analysis.

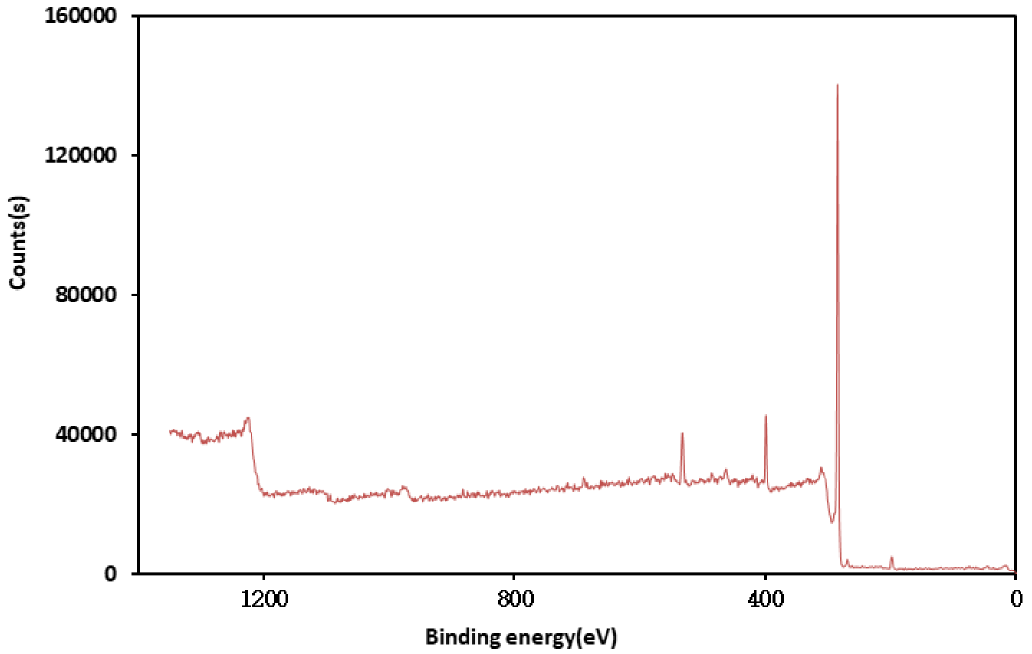

Figure S 1. XPS Analysis of the Ru-MOFs.

The samples were dispersed on the conductive tape. The SEM images were recorded on Inspect F50, FEI.

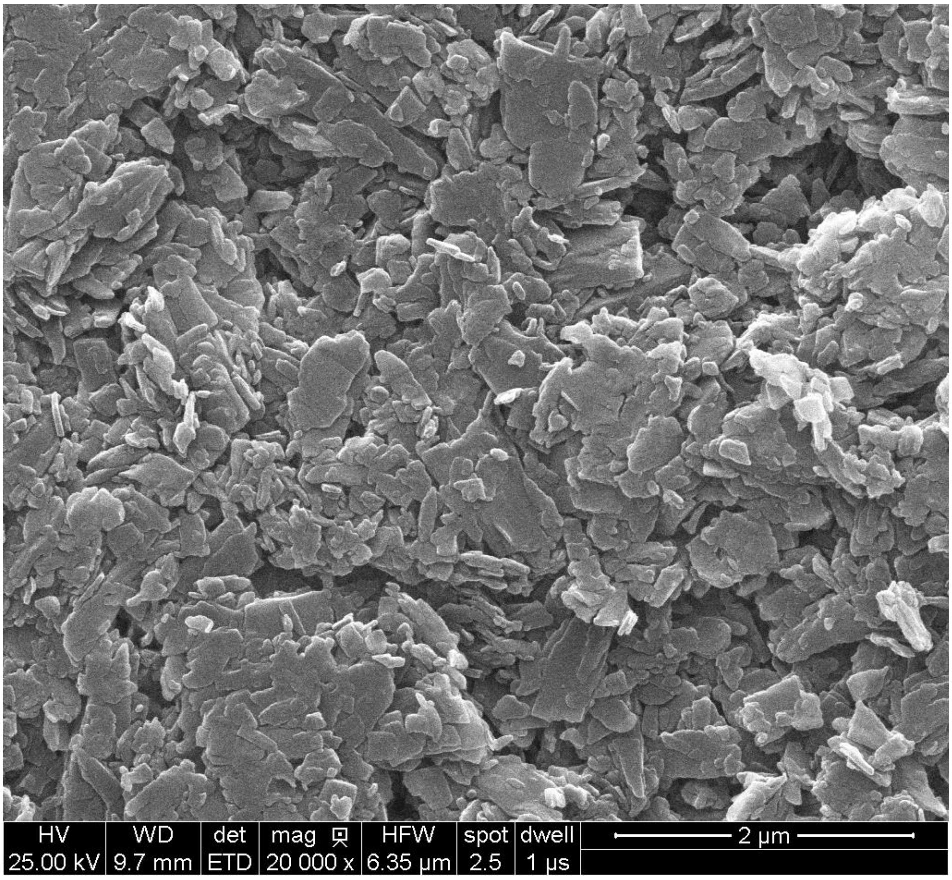

Figure S 2. SEM Image of the Ru-MOFs.

The transmission electron microscopy (TEM), high resolution transmission electron microscopy (HRTEM) images and selected area electron diffraction (SAED) were recorded on Talos F200X, Thermo Scientific. The EDS was analyzed by Super X, FEI.

Figure S 3. TEM Image of the Ru-MOFs.

As exhibited in **Figure S 4**, there are a few lattice plane in the HRTEM Image.

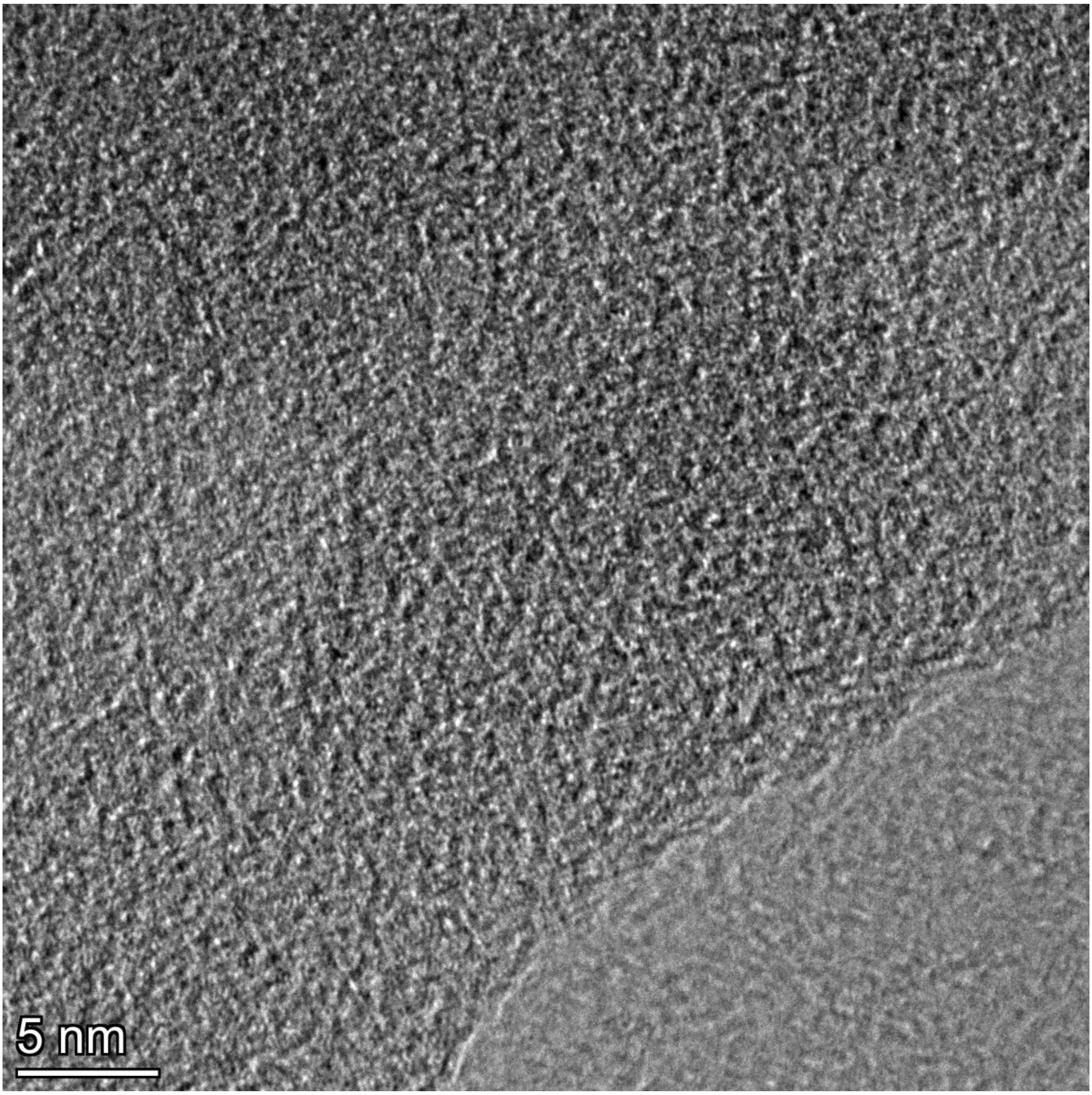

Figure S 4. HRTEM Image of the Ru-MOFs.

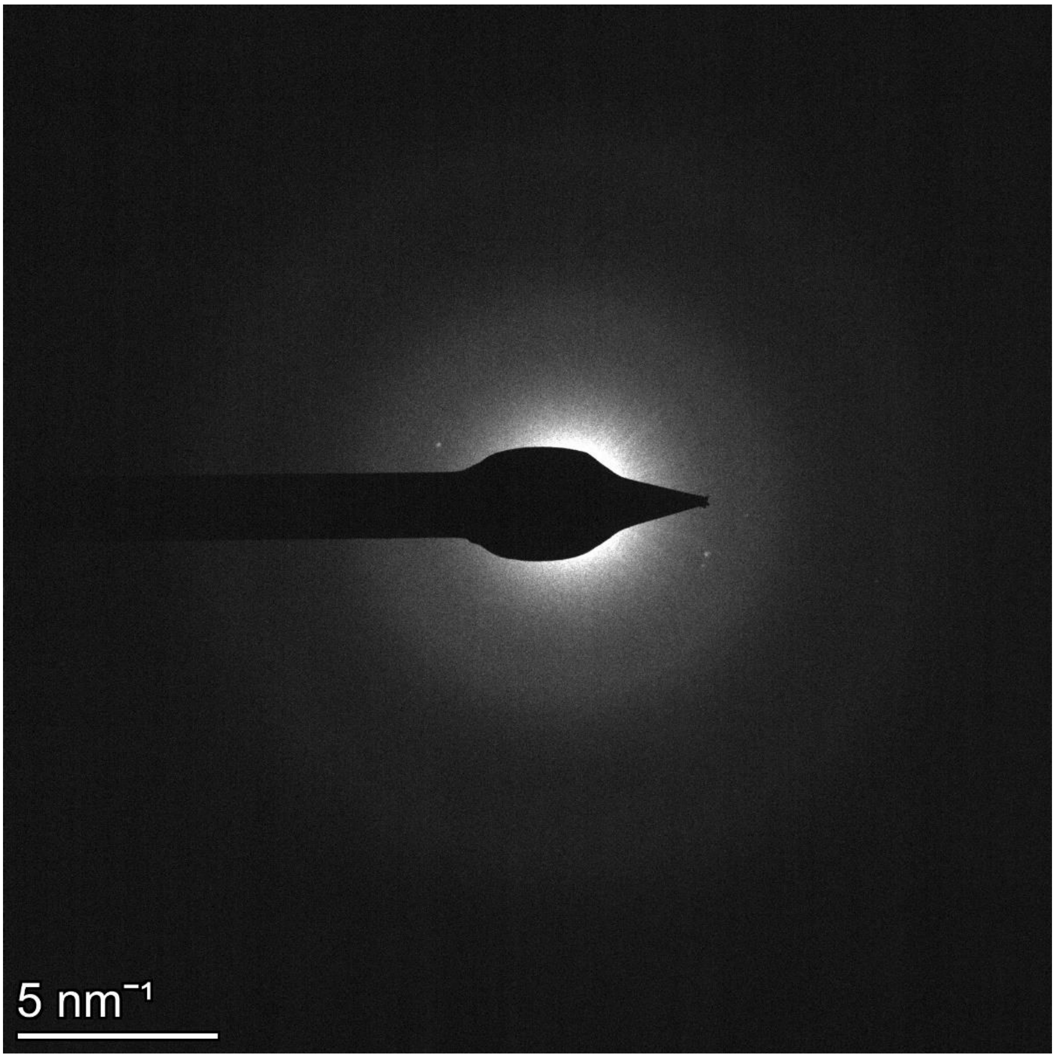

Figure S 5. SAED of the Ru-MOFs.

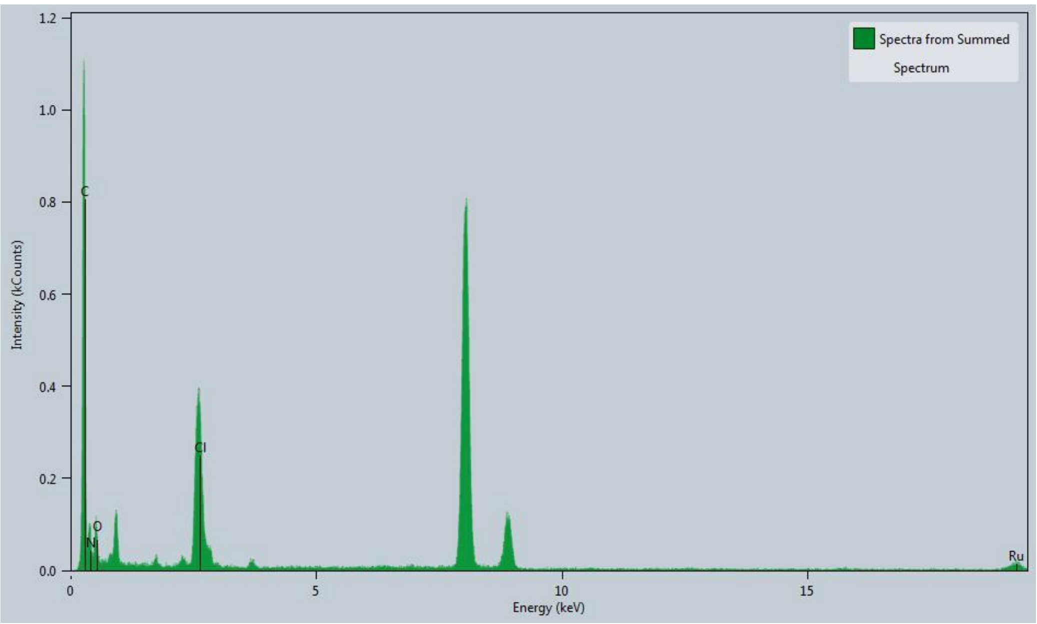

Figure S 6. EDS Analysis of the Ru-MOFs.

Table 1. Spectra from Summed-Background

Z	Element	Family	Atomic Fraction (%)	Atomic Error (%)	Mass Fraction (%)	Mass Error (%)	Fit error (%)
6	C	K	80.88	5.89	54.50	2.73	1.56
7	N	K	2.96	0.64	2.33	0.48	3.34
8	O	K	3.65	0.78	3.28	0.68	1.97
17	Cl	K	8.43	1.65	16.77	3.16	0.37
44	Ru	K	4.08	0.68	23.13	3.63	1.44

The EDS analysis was performed by Super X during the HRTEM test, it could estimate the main element content of the Ru-MOFs. As in the **Figure S 6** and **Table 1**, the ruthenium content is 23.13 wt%, which is close to the theoretical content of ruthenium in Ru-MOFs. The O in the **Table 1** is from the carbon film of the copper mesh during the HRTEM analysis. Because the Ru-MOFs sample is dispersed on the copper mesh before the HRTEM test.

The pore size distributions and average pore diameter of the catalyst were analyzed by the BJH nitrogen adsorption and desorption method.

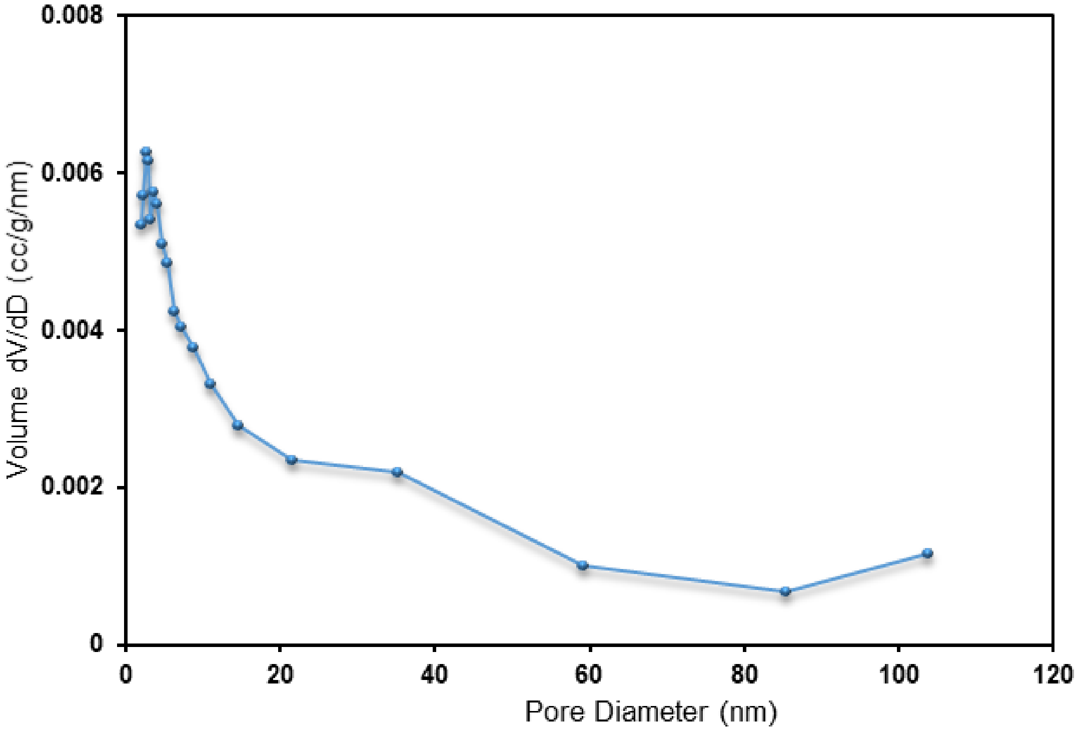

Figure S 7. The pore size distributions analyzed by the BJH nitrogen adsorption method.

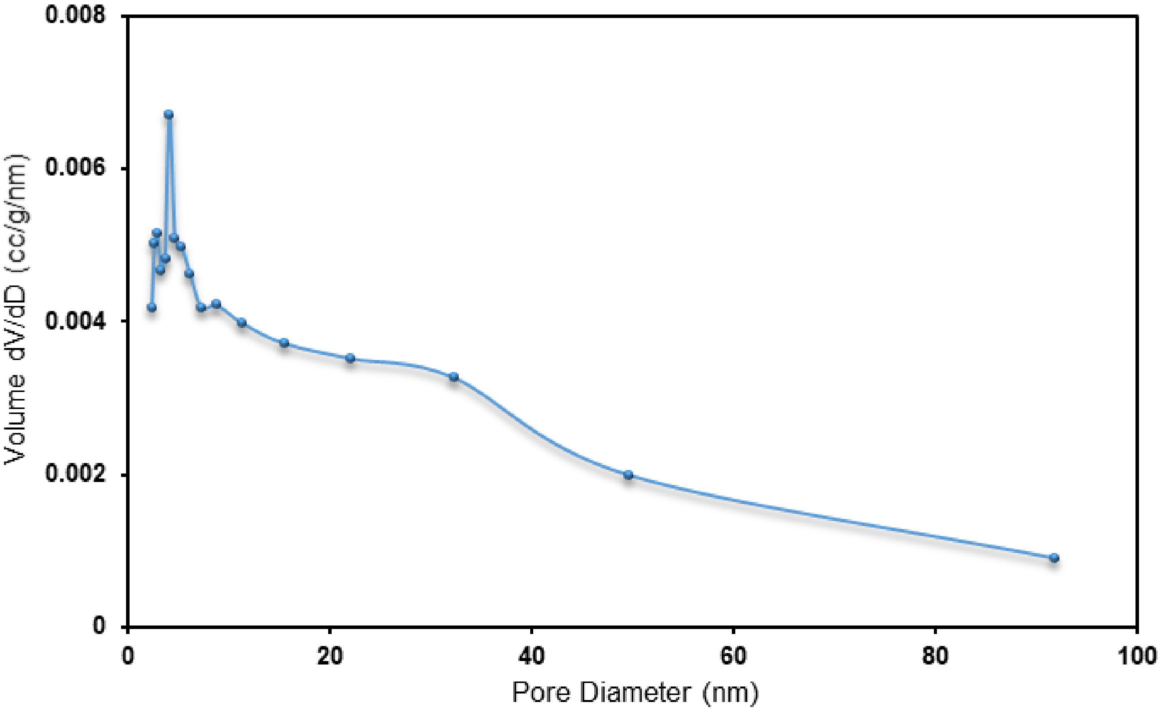

Figure S 8. The pore size distributions analyzed by the BJH nitrogen desorption method.

SI-4. Experiments for hydrogen production from methanol.

Representative experiment: 2 mg Ru-MOF were added in a 25 mL flask which contained 5 mL phosphate buffer and 3.09 mM NAD^+. Then the 60 U ADH were added in the suspension after the catalyst fully dispersed by ultrasonic. The flask was connected to a U-tube containing colored solution. The nitrogen was blow into the total device for more than 10 minutes, replaced the air inside. At last, the methanol was injected into the solution after the flask is heated to preset temperature. The methanol concentration is 400mM. The gas content was analyzed by the GC.

The generated gas during the methanol reforming was analyzed by GC-G5 (Beijing Persee General Instrument CO. Ltd). The gas chromatography was assembled with TDX-1 column, Porapak Q column, FID, TCD and methanizer, N_2 as carrier gas. We used the GC-TCD to detect the hydrogen and carbon dioxide from the room temperature methanol reforming and formaldehyde decomposition.

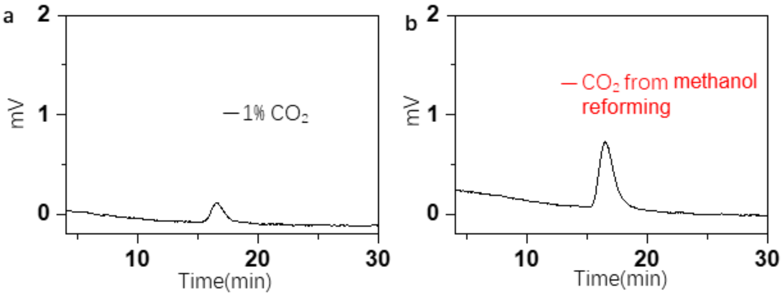

Figure S 9. CO_2 Measurement by Gas Chromatography (GC-TCD). (a) 1% CO_2 sample. (b) generated CO_2 gas during the methanol reforming.

SI-5. The Activity of Ru-MOFs for HCHO decomposition and NADH dehydrogenation.

Typical experiment for formaldehyde decomposition. Firstly, the 10 mg Ru-MOFs were added in a 25 mL flask which containing 10 mL phosphate buffer. The heterogeneous catalyst was fully dispersed in phosphate buffer by ultrasonic. Then the flask was connected to a graduated U-tube containing colored solution. Purged the catalytic reactor with nitrogen for more than 10 minutes, replaced the air inside. At last, 4.2 mL 37 wt% formaldehyde was injected into the phosphate buffer after the flask was heated to preset temperature. The reaction solution kept stirring by magnetic stirring bar. The generated gas could lead to the liquid level variation in the U-tube during the formaldehyde catalytic decomposition. This liquid level variation could be recorded by a digital camera, and help us gain the gas production rate. The temperature for volume measurement kept at 20 ℃.

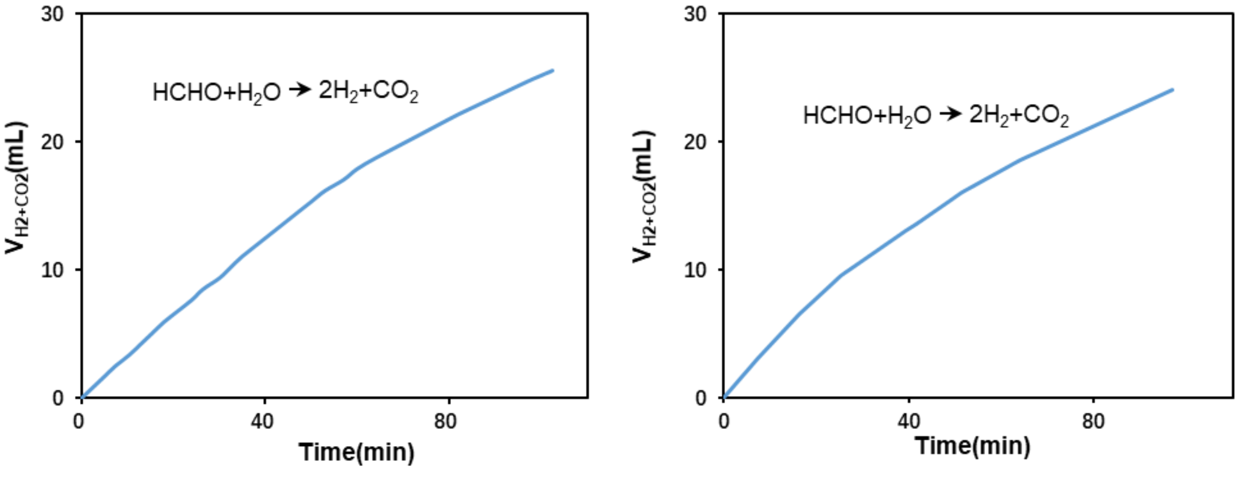

Figure S 10. Volume of Evolved Gas versus Reaction Time during 4 M Formaldehyde Decomposition over 10 mg Ru-MOFs at 40 ℃.

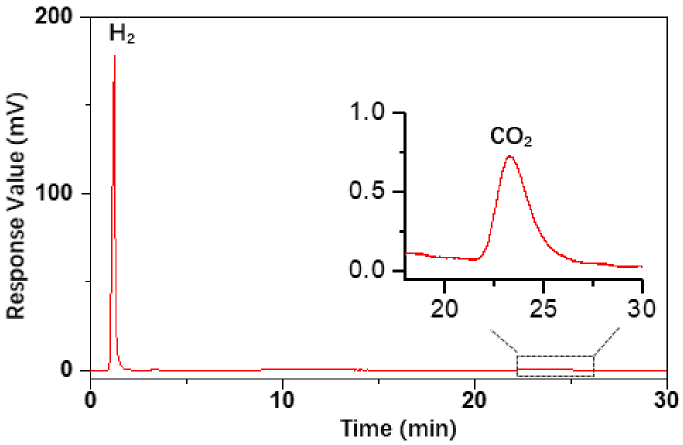

Figure S 11. GC-TCD analysis of the initial evolved gas from formaldehyde decomposition

TOF Calculations for HCHO decomposition. As exhibited in the **Figure S 11**, little carbon dioxide was detected by GC during the initial 30 minutes of reaction, so we calculated the TOF of the formaldehyde decomposition based on the chemical **Reaction (1)**.

$$HCHO + H_2O \rightarrow HCOOH + H_2$$ **Reaction (1)**

The TOF was calculated by **Equation 1**. The water vapor was neglected.

$$TOF=\frac{V_{H2}/(t*V_{m,20^{\circ}C})}{n_{(Ru)}}$$ **Equation 1**

V_{H2} was the volume of hydrogen which is generated during the initial 0.5 hour, t was 0.5 h. $n_{(Ru)}$ was the molar number of ruthenium. The ruthenium content of the Ru-MOFs was 23.7 wt% which was determined by Agilent 720 ICP-OES. The $V_{m,20^{\circ}C}$ was calculated by van der Waals equation of hydrogen.[1]

$$V_{m,20^{\circ}C}= \frac{RT}{p}+b-\frac{a}{RT} = 24\ L/mol$$ **Equation 2**

R is 8.3145 m^3 Pa mol^{-1} K^{-1}, T is 293.15 K, p is 101325 Pa, b is 26.7×10^{-6} $m^3\cdot mol^{-1}$, a is 2.49×10^{-10} $Pa\cdot m^3\cdot mol^{-2}$.

The Ru-MOFs also show high catalytic selectivity for the formaldehyde decomposition. As exhibited in the **Figure S 12**, carbon monoxide content is less than 10 ppm in the evolved gas. Actually, the formaldehyde decomposition is the only reaction which may produce the CO among the ADH induced methanol reforming. Attributing to the high catalytic selectivity for the formaldehyde decomposition, thus little CO will generate during the ADH induced methanol reforming.

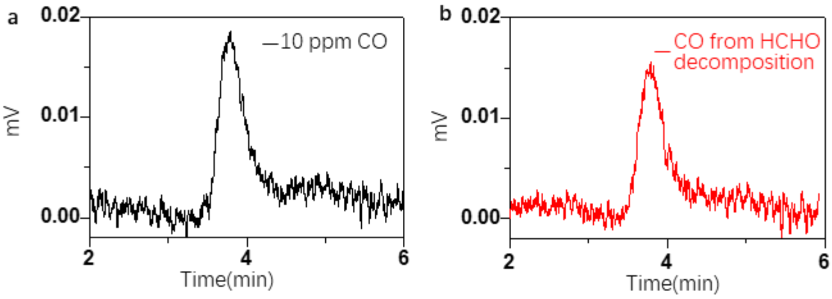

Figure S 12. Gas Chromatogram of CO using the FID Detectors and Methanizer. (a) 10 ppm CO sample. (b) generated CO during the formaldehyde decomposition.

Typical experiment for NADH dehydrogenation. Transferred 9 mL phosphate buffer and 2 mg Ru-MOFs in a 25mL flask. The flask was connected to a graduated U-tube containing colored solution. Purged the catalytic system with nitrogen for air replacement. Then 1mL 4 mM NADH solution was injected into the phosphate buffer after the flask was heated to preset temperature. The reaction solution kept stirring by magnetic stirring bar. We analyzed the NADH concentration by the UV-vis every 5 minutes during the NADH dehydrogenation.

SI-6. Activity of ADH measured by UV-Vis.

UV-absorption and enzymatic reaction kinetics were recorded by Shimadzu UV-2600. Typically, 700μL phosphate buffer was added in the quartz cell. The phosphate buffer contained 10 U ADH and 1.09 mM NAD$^+$. Then the 10 uL methanol was transferred into the quartz cell. The UV-absorption was recorded as soon as the reaction solution was shaken well. The generated NADH would leading to the increasing of the UV-vis absorption at 340nm during the methanol dehydrogenation. The methanol dehydrogenation rate is determined by the NADH variation.

$$CH_3OH+NAD^+ \rightarrow H^++NADH+HCHO$$

The ADH is the protein essentially, its activity may decrease drastically in the strong acid or basic solution. As exhibited in the **Figure S 13**, the methanol dehydrogenation rate 1.3 μmol h^{-1} kU^{-1} and 5.9 μmol h^{-1} kU^{-1} in 0.1 M HCl or 0.1 M NaOH solution respectively.

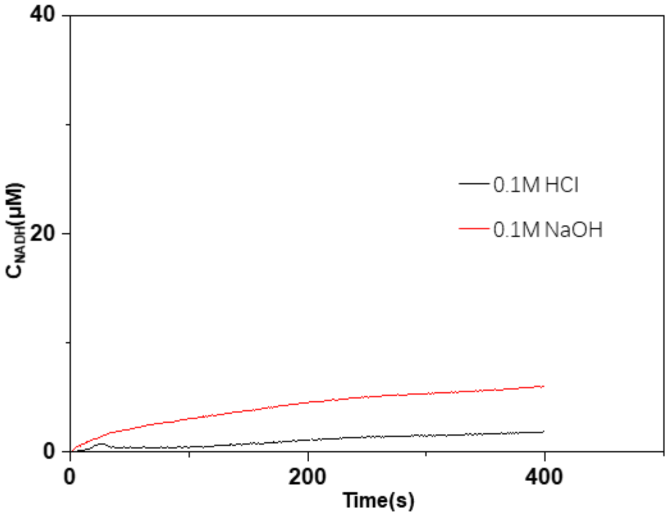

Figure S 13. Methanol dehydrogenation by ADH in 0.1 M HCl or 0.1 M NaOH solution respectively. Condition: 10 U ADH, 350 mM CH_3OH, 1.09 mM NAD$^+$.

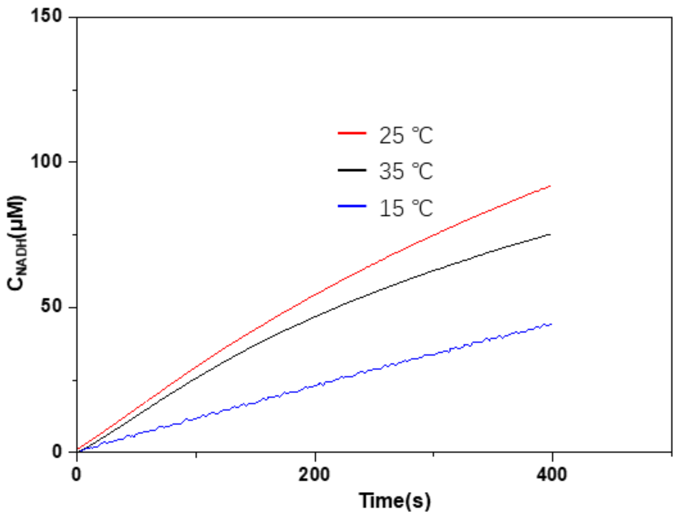

Figure S 14. Methanol Dehydrogenation by ADH at 15°C, 25°C and 35°C respectively. Condition: 10 U ADH, 350 mM CH_3OH, pH=8.2, 1.09 mM NAD^+.

SI-7. Effect of Ru-MOFs on ADH.

We study the methanol dehydrogenation kinetics of the ADH by the UV-vis. The generated NADH will leading to the increasing of the UV-vis absorption at 340nm during the methanol dehydrogenation. We mix the 20 U ADH with the Ru-MOFs in the 700μL phosphate buffer. After 24 hours, we test the ADH activity. The blue line in **Figure S 15** exhibit the generated NADH versus time trajectory during the methanol dehydrogenation, indicate the ADH could keep the activity for the methanol dehydrogenation. 3000 seconds later, the reaction will begin to reach a balance state.

We mix the 20 U ADH with the 50μM Ru(p-Cymene)$(NH_3)Cl_2$ in the 700μL phosphate buffer. Then 1 mM NAD^+ and 10 μL methanol added in the phosphate buffer for testing the ADH activity. The ADH kinetics was recorded after reaction solution was shaken well. As exhibited in the brown line of **Figure S 15**, no NADH would generate during the methanol dehydrogenation. It indicates the ADH has been inactivated.

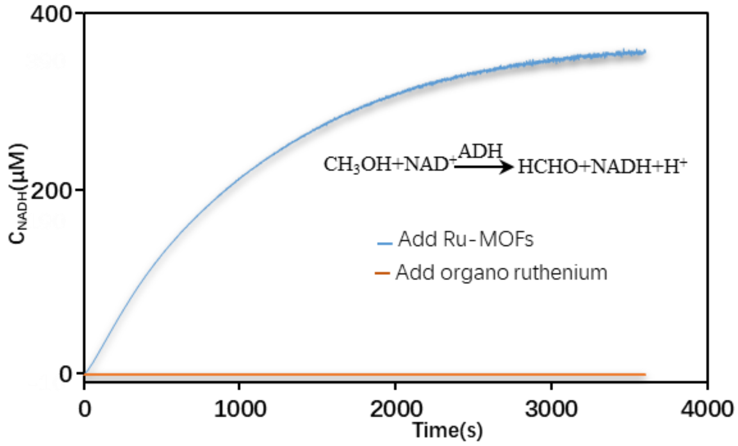

Figure S 15. The Trajectory for NADH Concentration Versus Reaction Time during Methanol Dehydrogenation under Different Condition. The brown line: 50μM Ru(p-Cymene)(NH_3)Cl_2 was added in ADH solution.

SI-8. The Products during NADH Dehydrogenation.

The NADH could be dehydrogenated over the Ru-MOFs. Typically, 2mg Ru-MOFs is dispersed in the 9 mL phosphate buffer by ultrasonic dispersion. The reaction flask is connected to the graduated U-tube containing colored solution. Purged the catalytic reactor with nitrogen for more than 10 minutes, replaced the air inside. At last, quantitative high-concentration NADH was injected into the phosphate buffer after the flask was heated to preset temperature. The NADH concentration is 400μM in the phosphate buffer. The reaction solution kept stirring by magnetic stirring bar. We analyzed the NADH concentration by the UV-vis every 5 minutes during the NADH dehydrogenation. The hydrogen also can be detected by GC-TCD during the NADH dehydrogenation.

SI-9. Calculation of the Hydrogen Production Rate.

$$r_{H2}=\frac{v_{H2}}{n_{Ru}}$$

r_{H2} is the hydrogen production rate during the methanol reforming, which is evaluated by the ruthenium dosage. The unit is mmol h^{-1} mol^{-1} $_{(Ru)}$ or μmol h^{-1} mol^{-1} $_{(Ru)}$.

v_{H2} is calculated by fitting the trajectory for the amount of generated hydrogen versus reaction time, is equal to the slope of the trajectory. The unit is μmol h^{-1}.

n_{Ru} is the amount of ruthenium.

$$n_{Ru}=\frac{0.237*m_{cata}}{101.1}$$

m_{Ru} is the dosage of the Ru-MOFs in the reaction solution. The 101.1 is the relative atomic mass of ruthenium. The ruthenium content of Ru-MOFs is 23.7 wt%, which is determined by Agilent 720 ICP-OES.

For example, the yellow color trajectory in **Figure 4** is the generated hydrogen versus reaction time when the pH of the solution is 7.5. The slope of the trajectory is 0.5. The dosage of Ru-MOFs is 0.002 g during the methanol reforming. So the r_{H2} is 107000 μmol h^{-1} mol^{-1} $_{(Ru)}$ or 107 mmol h^{-1} mol^{-1} $_{(Ru)}$.

SI-10. Blank Reactions for Hydrogen Production from Methanol Reforming.

Every reactant is important for the hydrogen production from the ADH- induced methanol reforming, As exhibited in the **Figure S 16**, **Figure S 17** and **Figure S 18**, no hydrogen is detected from the methanol reforming in in the absence of ADH, NAD^+ and Ru-MOF.

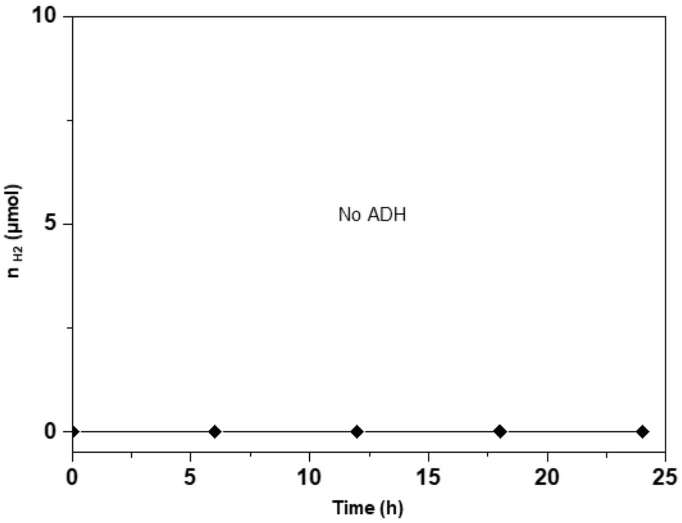

Figure S 16. H_2 production in absence of ADH.

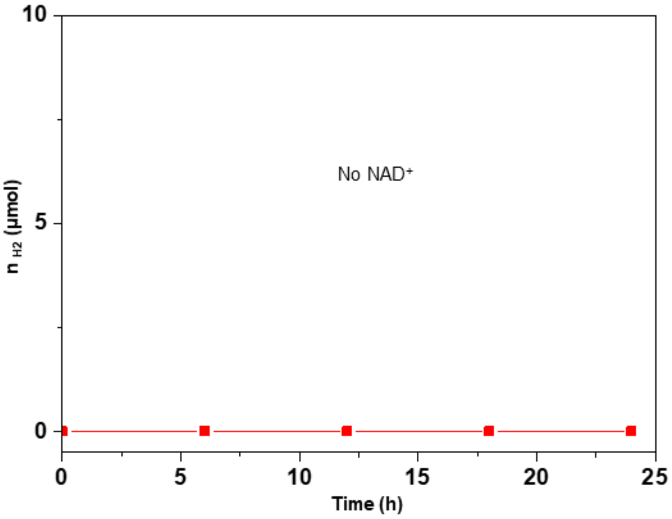

Figure S 17. H_2 production in absence of NAD^+.

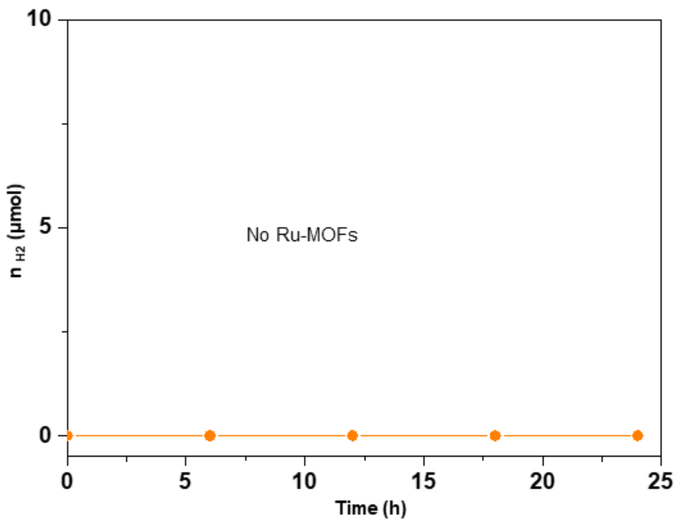

Figure S 18. H_2 production in absence of Ru-MOF.

SI-11. Activity Test of the ADH and Ru(p-Cymene)NH_3Cl_2 after They Employed in Methanol Reforming in Figure 3a.

The absence of H_2 production due to the deactivation of ADH under the brown line condition of **Figure 3a**. We analyzed the ADH and Ru(p-Cymene)NH_3Cl_2 after they employed in methanol reforming in **Figure 3a**. We transferred 2mL reaction solution in the cuvette, and added 1 mL 4 mM NAD^+ and 30 μL methanol in the solution. Then gain the enzyme kinetics by UV-vis. As exhibited in the **Figure S 19**, the ADH lose the activity for methanol dehydrogenation, no NADH will generate through the reaction.

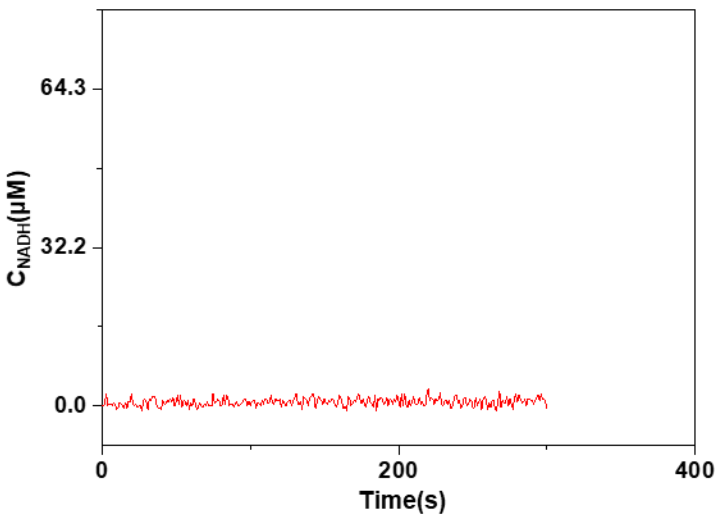

Figure S 19. Activity Test of the ADH after Employed in Brown Line Conditions of Figure 3a.

We transferred 4 mL reaction solution in flask, then added 1 mL 5 M formaldehyde solution after the flask was heated to 50℃. The solution could generate the gas, the gas is hydrogen and carbon dioxide.

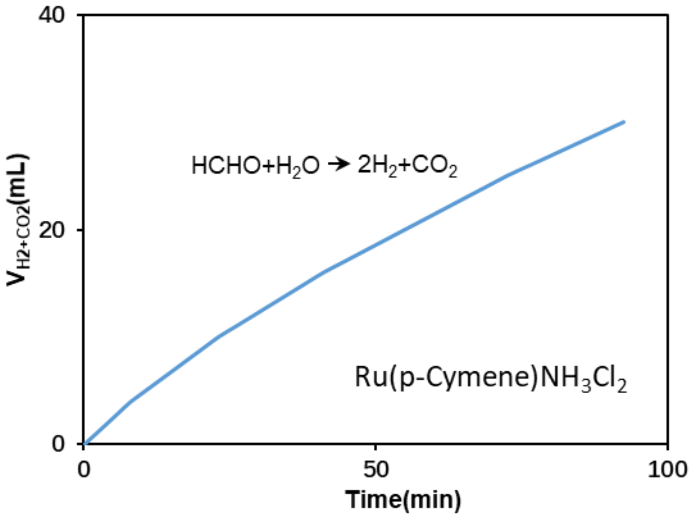

Figure S 20. Activity Test of the Ru(p-Cymene)NH_3Cl_2 after Employed in Brown Line Conditions of Figure 3a.

SI-12. XRD pattern of the Ru-MOFs

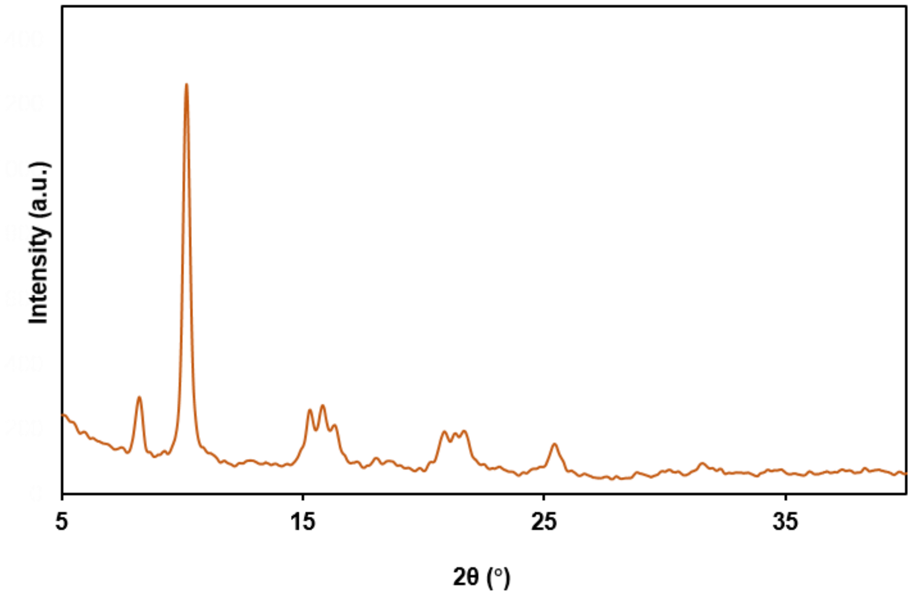

Figure S 21.XRD pattern of the Ru-MOFs after it employed in methanol reforming.

References

(1) Wang, Z.; Lu, S. M.; Li, J.; Wang, J.; Li, C. Unprecedentedly High Formic Acid Dehydrogenation Activity on An Iridium Complex with An N,N'-diimine Ligand in Water. *Chemistry–A European Journal* **2015,** 21 (36), 12592-12595.